



Signal amplification in capillary electrophoresis based chemiluminescent immunoassays by using an antibody–gold nanoparticle–DNAzyme assembly

Min Shi^a, Shulin Zhao^{a,*}, Yong Huang^a, Limin Zhao^a, Yi-Ming Liu^b

^a Key Laboratory for the Chemistry and Molecular Engineering of Medicinal Resources (Ministry of Education), College of Chemistry and Chemical Engineering, Guangxi Normal University, Guilin 541004, China

^b Department of Chemistry and Biochemistry, Jackson State University, 1400 Lynch St., Jackson, MS 39217, USA

ARTICLE INFO

Article history:

Received 29 October 2013

Received in revised form

9 February 2014

Accepted 15 February 2014

Available online 28 February 2014

Keywords:

Capillary electrophoresis

Gold nanoparticles

Chemiluminescent immunoassays

Signal amplification

Carbohydrate antigen 19-9

ABSTRACT

A signal amplification strategy based on antibody–gold nanoparticle–DNAzyme assembly in capillary electrophoresis based chemiluminescent immunoassays (CE-CLIA) was developed. In this CE-CLIA, antibody–AuNP–G-quadruplex/hemin was incubated with limited amount of antigen, and the formed immunocomplex and unreacted antibody–AuNP–G-quadruplex/hemin were then separated by CE and detected by CL. Due to the strong CL catalytic ability of G-quadruplex/hemin DNAzyme and a high loading ratio of DNAzyme on each AuNP, the assay was very sensitive. By taking carbohydrate antigen 19-9 (CA19-9), one of the most important carbohydrate tumor marker as the model analyte, the proposed CE-CLIA method for CA19-9 detection showed a linear range from 0.025 to 1.00 U/mL with a detection limit of 0.016 U/mL (signal/noise=3), which was more sensitive than the methods previously reported for CA19-9 quantification. The method was applied to quantify CA19-9 in human serum samples, and analytical results were in a good agreement with those obtained by using an established ELISA method.

© 2014 Elsevier B.V. All rights reserved.

1. Introduction

Capillary electrophoresis (CE) is an established microseparation technique, which provides advantages of high separation efficiency, short analysis time, small analyte consumption, simplicity, and almost no environmental pollution [1]. Chemiluminescence (CL) detection is known as an attractive detection scheme in CE [2] due to its low background nature, high sensitivity, a wide linearity range, and simple instrument requirements. Thus, the CE-CL analytical technique has been deployed to determine various types of biomedical molecules in complex samples such as serum and other physiological fluids [3–5]. Unfortunately, CE-CL assay lacks high sensitivity compared with conventional CL assay techniques because only a very small amount of sample was introduced into the system for analysis [6]. This technique was difficult for the detection of trace substance in biological samples. Therefore, the development of highly sensitive detection schemes for CE-CL assay is necessitated [7].

Gold nanoparticles (AuNPs) have attracted attention in the last few years, owing to their unique structural, electronic, magnetic, optical, and catalytic properties, which have made them a very

attractive material for biosensor systems and bioassays [8,9]. Recently, AuNPs have been used as a catalytic label for amplified detection of DNA and proteins [10,11], and AuNPs functionalized with nucleic acids were employed as versatile labels for the optical detection of DNA and proteins [12,13]. Based on the enhanced effect, AuNPs have also been used as labels for amplified electrochemical detection [14,15], quartz crystal microbalance detection [16,17], CL detection [18,19] and resonance Raman scattering-based detection [20]. Although many AuNP enhancement-based methods have been reported for sensing of various targets, few methods are currently available for amplified CE-CL assay.

G-quadruplex-based DNAzymes formed by hemin and DNA G-quadruplexes are a kind of nucleic acid enzymes with the peroxidase-like activity. Compared with protein enzymes, DNAzymes are more stable and less expensive to produce, and can be denatured and re-natured many times without losing their biological activity. Therefore, G-quadruplex DNAzymes have increasingly received attention in the last decade, and are used in various applications including colorimetric detection of nucleic acids and proteins [21,22], colorimetric detection of metal ions [23], fluorimetric detection of DNA [24] and genetically modified organisms [25], and electrochemical detection of nucleic acids [26]. However, to the best of our knowledge there has been no report on using a peroxidase-mimicking DNAzyme and AuNPs to enhance CE-based chemiluminescent immunoassays (CE-CLIA).

* Corresponding author. Tel.: +86 773 5856104; fax: +86 773 5832294.

E-mail address: zhaoshulin001@163.com (S. Zhao).

In this work, an assembly of antibody–AuNP–DNAzyme was designed to explore a novel strategy for signal amplification in CE-CLIA. The DNAzyme used in the study was prepared by embedding a hemin in a guanine-rich DNA strand. This G-quadruplex/hemin DNAzyme mimicked peroxidase enzymes catalyzing the CL reaction between luminol and H_2O_2 , one of the most widely used CL reaction in immunoassays. Because a high loading ratio of the CL catalytic DNAzyme over the signal antibody on an AuNP, analytical signal amplification was achieved. Characterization of the assembly prepared was carried out by UV–vis and Circular Dichroism (CD) spectra. The effects of the assembly composition on catalyzing luminol– H_2O_2 CL reaction were studied. Carbohydrate antigen 19-9 (CA19-9), one of the most important carbohydrate tumor markers, was taken as the model analyte. Assay conditions and the analytical figures of merit were investigated. The proposed CE-CLIA assay was preliminarily validated by quantifying CA19-9 in human serum samples.

2. Experimental

2.1. Apparatus and reagents

CE-CL experiments were carried out using a laboratory-built CE-CL system as described previously [27–29]. Absorption spectra were recorded on a TU-1901 UV–vis spectrophotometer (Beijing Purkinje General Instrument Co., Ltd., Beijing) at room temperature. CL spectra were measured with a LS-55 luminescence spectrometer (Perkin-Elmer, USA). CD spectra were recorded on a J-810 Circular Dichroism spectrophotometer (JASCO, Japan).

CA19-9 was purchased from Beijing Yuande Biomedical Engineering Co., Ltd. (Beijing, China). Luminol was purchased from Fluka (Buchs, Switzerland). DNA (5'-SH-AAAAAAGGGTTGGGCGG-GATGGGT-3') was synthesized by Shanghai Sangon Biotechnology Co., Ltd. (China). Hemin and Bovine Serum Albumin (BSA) were purchased from Sigma Chemicals (St. Louis, MO). Tetrachloroaurate (III) tetrahydrate ($\text{AuCl}_3 \cdot \text{HCl} \cdot 4\text{H}_2\text{O}$, 48%, w/w), sodium citrate, Tris(2-carboxyethyl)phosphine (TCEP), Triton X-100, Tween 20, hydrogen peroxide (H_2O_2 , 30%), sodium dodecyl sulfate (SDS) and tris(hydroxymethyl) aminomethane (Tris) were obtained from Sinopharm Chemical Reagent Co., Ltd. (Shanghai, China). All other chemicals used in this work were of analytical grade. Water was purified by employing a Milli-Q plus 185 equip from Millipore (Bedford, MA), and used throughout the work.

CA19-9 and antibody solutions were prepared by dissolving the reagents in 0.01 M phosphate buffered saline (PBS; 0.1 M NaCl, 10 mM phosphate, pH 7.4). Blocking buffer solution consisted of a 0.01 M PBS solution (pH 7.4) with 1% (w/v) BSA (BSA in the PBS can block the active point of AuNPs and avoid unspecific adsorption onto AuNPs). DNAzyme reaction buffer solution consisted in a 20 mM Tris–HCl (pH 7.4) with 0.03% (w/v) Triton X-100 and 20 mM KCl. Hemin stock solution (5 mM) was prepared in dimethyl sulfoxide and stored in dark at -20°C , and diluted to the required concentration with DNAzyme reaction buffer solution. The stock solution consisted of a 0.01 M PBS solution (pH 7.4) with 0.003% (w/v) Triton X-100 and 10 mM KCl [30]. The electrophoresis buffer was 10 mM sodium borate solution at pH 10.0 containing 0.2% (v/v) Tween 20. CL reaction buffer was 20 mM sodium bicarbonate solution at pH 11.0 containing 1.0 mM luminol, and 50 mM H_2O_2 .

2.2. Preparation of AuNPs

AuNPs were prepared according to the literature method [31] with slight modification. Briefly, 100 mL of 0.01% (w/v) HAuCl_4 solution was transferred to a flask and heated to boil with vigorous

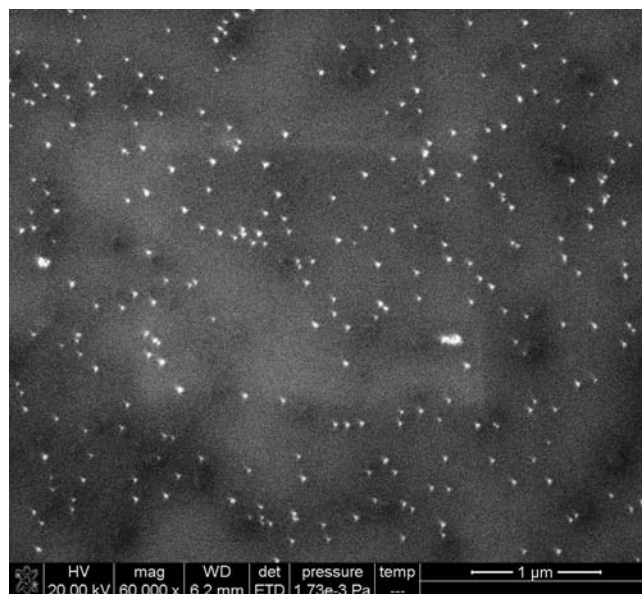


Fig. 1. SEM image of bare AuNPs.

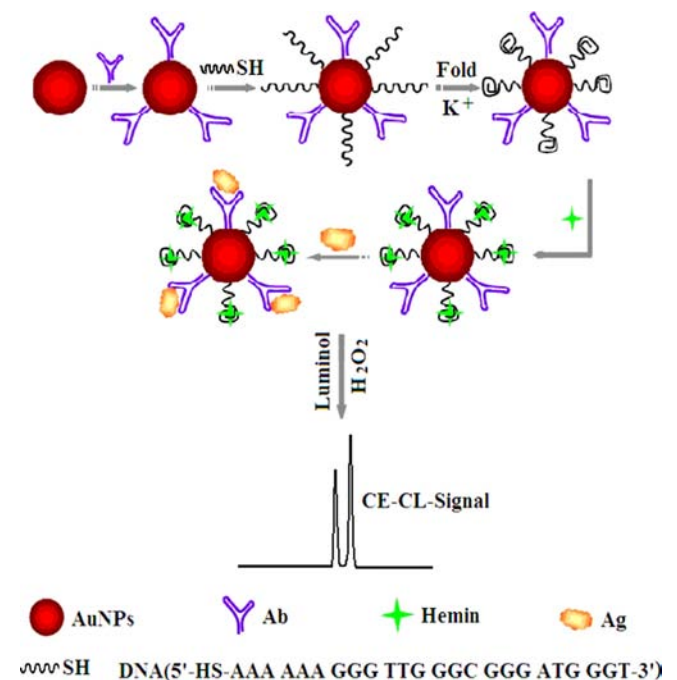
stirring, and 1.5 mL of 1.0% (w/v) trisodium citrate solution was quickly added to the boiling solution. The color of the solution changed from pale yellow to wine red in a few seconds, indicating the formation of AuNPs. The solution was refluxed for 30 min. The solution was then cooled to room temperature, and stored at the 4°C before use. The size and monodispersity of AuNPs prepared were determined by using a JEOL 100CX transmission electron microscope (SEM). SEM imaging revealed that the average diameter of AuNPs synthesized in this work was about 25 nm (Fig. 1).

2.3. Preparation of antibody–AuNP–G-quadruplex/hemin assembly

The anti-CA19-9 antibody–AuNP–DNAzyme assembly was prepared according to a procedure previously reported with minor modifications [32]. Scheme 1 illustrates the preparation. The pH of a colloidal AuNP solution was adjusted to 9.0 by adding NaOH, then $10\ \mu\text{L}$ of $1\ \text{mg mL}^{-1}$ anti-CA19-9 antibody (Ab) was added to 1 mL of the AuNP solution, followed by an incubation for 4 h at room temperature under gentle stirring. Subsequently, $10\ \mu\text{L}$ of a $100\ \mu\text{M}$ SH-DNA solution was mixed with $10\ \mu\text{L}$ of 0.03 mM TCEP solution (pH 7.4). 1 h later, the mixture was added to the resulting Ab-attached AuNPs and incubated for 16 h. After a salt-stabilization in 0.1 M NaCl, 1 mL of 5% BSA solution was added with stirring during a time period of 30 min to passivate the left active sites on AuNPs. The resulting solution was centrifuged at 20,000 rpm at 4°C for 20 min. The obtained functional AuNPs were re-suspended in 1 mL DNAzyme reaction buffer solution. Finally, a 0.3-mL portion of $5\ \mu\text{M}$ hemin was then added to the solution. After stirring for 1.5 h, the excess of antibody, DNA, and hemin were removed by centrifugation (20,000 rpm, 20 min at 4°C). The AuNPs fraction was redispersed in the stock solution, which was repeated for further purification. The solution of the formed Ab–AuNP–G-quadruplex/hemin assembly was stored in a refrigerator at 4°C before use.

2.4. Preparation of human serum samples

Human blood samples were kindly provided by the No. 5 People's Hospital (Guilin, China). Human blood samples were centrifuged at 20,000 rpm for 15 min to remove erythrocytes. Subsequently, the supernatant was diluted with PBS appropriately before being analyzed.

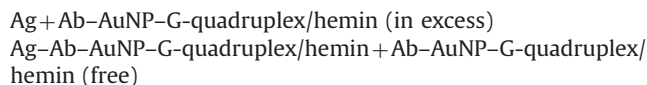


Scheme 1. Schematic illustration of the developed CE-based noncompetitive chemiluminescent immunoassay with signal amplification enabled by antibody-AuNP-DNAzyme assembly.

2.5. Immunoreaction procedure

CA19-9 and Ab-AuNP-G-quadruplex/hemin solutions were diluted to the appropriate concentrations with 0.01 M PBS (pH 7.4). For noncompetitive immunoassay, a 10 μ L Ab-AuNP-G-quadruplex/hemin solution and a series of 10 μ L CA19-9 solutions at different concentrations or samples were added to a 500 μ L microcentrifuge tube, and then the mixture solution was diluted with 0.01 M PBS (pH 7.4) to 100 μ L and incubated at 37 $^{\circ}$ C for 60 min.

The IA protocol was of non-competitive format and the immunoreaction was conducted as follows:



2.6. CE-CL determination

The capillary was preconditioned by flushing with 1 M NaOH for 30 min before the first use. Between two consecutive injections, the capillary was rinsed sequentially 0.1 M NaOH, water and running buffer for 5 min each. Samples were injected into the capillary by hydrodynamic flow at a height differential of 20 cm for 8 s. Separation voltage was 20 kV.

3. Results and discussion

3.1. Design and preparation of Ab-AuNP-G-quadruplex/hemin assembly for signal amplification in CE-CL immunoassay

G-quadruplex/hemin based DNAzymes exhibit catalytic activities similar to peroxidase enzymes, and therefore, they have the potential to be used as a new label for CL immunoassays.

In traditional enzyme immunoassays, usually a 1:1 ratio of enzyme to signal Ab is used. The detectable signal is directly proportional to the amount of Ab-Ag complex formed. In this work, we propose to use an assembly of the Ab and CL catalytic enzyme on an AuNP to enhance immunoassay sensitivity. The assembling allows creating a microenvironment where one signal Ab molecule is expressed by multiple CL catalytic enzyme molecules, thus achieving analytical signal amplification. Due to the intrinsic property of high surface-to-volume ratio, AuNPs can load numerous DNAzyme molecules with a relatively low content of Ab by controlling the amount of Ab added to AuNP solutions in the preparation of Ab-AuNP. An assembly with a low relative content of Ab reduces the binding ability of the assembly for the antigen in the immunoreaction, while with a high content of Ab limits the loading of DNAzyme on the nanoparticle surface, compromising CL signal amplification (Scheme 1). To achieve the maximum CL signal for CA19-9 at a certain concentration, assemblies prepared from Ab and HS-DNA solutions at various concentrations were tested. Results showed that using 1 mg mL⁻¹ Ab and 1.2 nM HS-DNA solutions produced the assembly exhibiting the strongest signal amplification.

3.2. Characterization of the Ab-AuNP-G-quadruplex/hemin assembly

UV-vis spectra were used to examine the binding of the Ab and DNAzyme to AuNPs. The UV-vis spectra of AuNP, Ab-AuNP conjugate, and Ab-AuNP-G-quadruplex/hemin assembly are shown in Fig. 2. The size of the AuNPs could be estimated to be 25 nm from the absorption peak at 526 nm (curve a), which was further confirmed by SEM (data shown below). Compared with AuNP, the UV-vis spectrum of antibody-AuNP conjugate showed a red shift of the absorption peak to 530 nm (curve b), indicating that a slight aggregation of the nanoparticles occurred after the binding of anti-CA19-9 antibody. Meanwhile, a 276 nm absorption peak appeared, which was corresponding to the typical protein absorption peak, indicating the successful loading of Ab onto AuNPs. After the guanine-rich DNA strand was attached on the surface of AuNPs, a strong absorption at approximately 267 nm appeared for Ab-AuNP-G-quadruplex/hemin (curve c), which was obviously stronger than the absorption peak of antibody-AuNP conjugate at 276 nm (curve b) due to the adsorption of the guanine-rich DNA strand, indicating the successful immobilization of G-quadruplex oligonucleotides on AuNPs. It is worth noting that there were no free Ab molecules in the Ab-AuNP conjugate

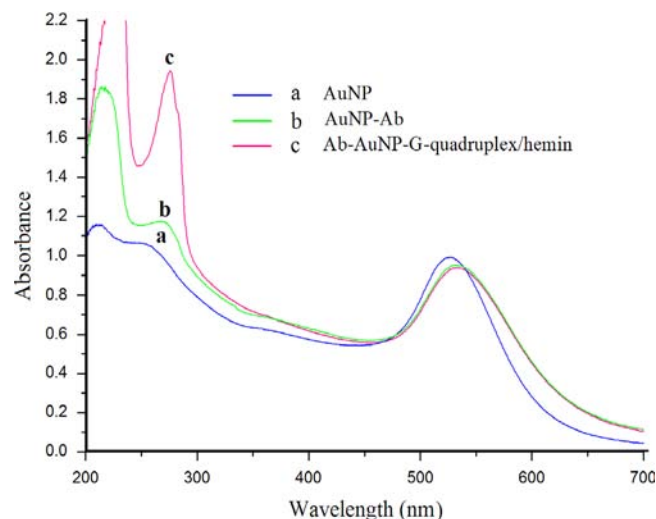


Fig. 2. UV-vis absorption spectra of AuNP (a), AuNP-Ab (b) and Ab-AuNP-G-quadruplex/hemin (c).

solution, and no free G-quadruplex/hemin in Ab–AuNP–G-quadruplex/hemin assembly solution. They were removed by ultracentrifugation during the preparation of respective solutions.

During the preparation of the assembly, G-quadruplex oligonucleotides were folded into a G-quadruplex so that hemin could be embedded to form a G-quadruplex/hemin DNAzyme. To investigate the formation of the G-quadruplex, CD spectra of G-quadruplex/hemin and Ab–AuNP–G-quadruplex/hemin were recorded (Fig. 3). After formation of the G-quadruplex/hemin complex, a positive peak at 265 nm and a negative peak at 245 nm were observed in the spectrum, indicating that G-quadruplex oligonucleotides successfully folded into a parallel G-quadruplex [33,34]. Ab–AuNP–G-quadruplex/hemin also showed two peaks near 265 nm and 245 nm, suggesting the formation of a G-quadruplex structure.

3.3. Luminol–H₂O₂ CL reaction catalyzed by Ab–AuNP–G-quadruplex/hemin assembly

CL spectra were recorded from luminol–H₂O₂ solutions with or without a catalyst. CL emission from a luminol–H₂O₂ solution without a catalyst was very low as can be seen from Fig. 4d.

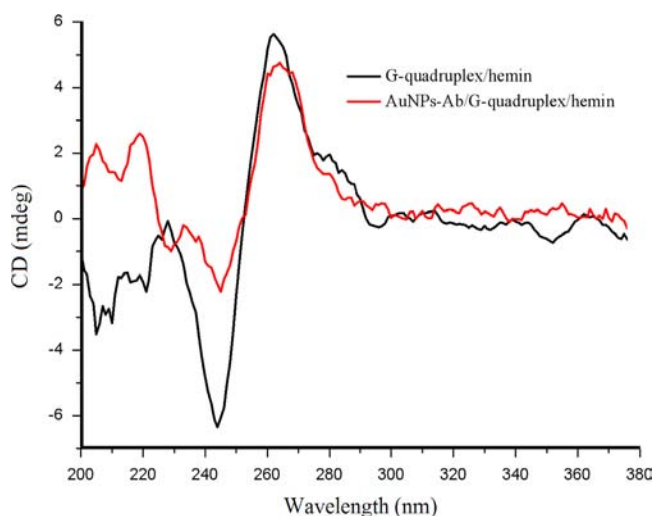


Fig. 3. CD spectra of G-quadruplex/hemin and Ab–AuNP–G-quadruplex/hemin.

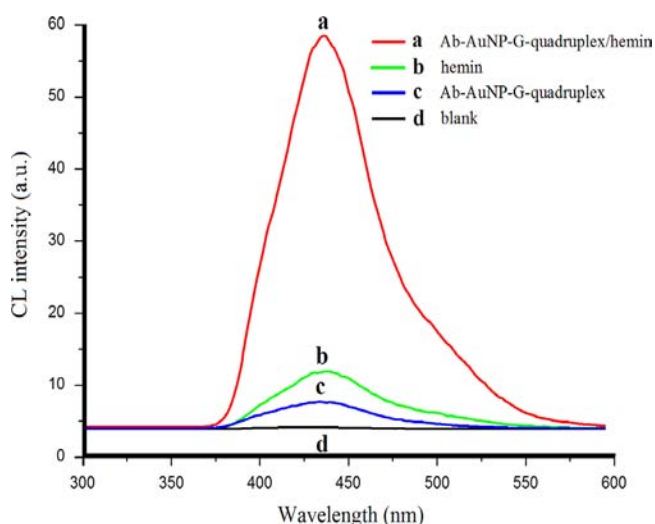


Fig. 4. CL spectra recorded from luminol–H₂O₂ solutions in presence of various catalytic components.

Introducing the guanine-rich DNA or hemin into the solution, the CL intensity did not change much in the wavelength range from 370 to 500 nm (Fig. 4c and b). Upon the addition of K⁺ and hemin into the luminol–H₂O₂ solution containing guanine-rich DNA–AuNP–antibody assembly, G-quadruplex/hemin DNAzyme was formed, resulting in a maximum CL emission at about 430 nm (Fig. 4a). It is worth noting that the CL emission had a maximum at the same wavelength as that of the HRP-catalyzed CL emission, indicating the DNAzyme catalyzed CL process had the same CL mechanism as the HRP catalyzed CL emission. By comparing Fig. 3a with Fig. 3b, one could see a much stronger catalytic ability of the Ab–AuNP–G-quadruplex/hemin assembly than that of free hemin. The strong ability resulted from both the high catalytic efficiency of DNAzyme due to less embedding of the activity center in the G-quadruplex structure than in macromolecular peptides of HRP [35] and the higher loading amount of DNAzyme on AuNPs due to its smaller size than HRP [32].

3.4. CL immunoassay

In order to achieve the maximal CL signal, effects of the CL reagent (luminol), oxidizer (H₂O₂), and the pH of CL reaction buffer (NaHCO₃ solution) on the CL intensity were investigated. In these experiments, the CL intensity (peak height) from assaying an Ab–AuNP–G-quadruplex/hemin solution was recorded. Test results indicated that the optimal luminol concentration was 1.0 mM (luminol concentration range tested was from 0.1 to 1.5 mM) and the optimal H₂O₂ concentration was 50 mM (5–70 mM concentration range was tested). The effects of pH value of NaHCO₃ solution was also investigated in a pH range of 9.0–12.0. The results indicated that the CL intensity increased with pH increase in the range of 9.0–11.0. After pH values were higher than 11.0, the CL intensity decreased sharply. Therefore, the post-column introduced CL reaction solution was buffered at 11.0. From these studies, CL reagent and oxidizer concentrations were selected to be 1.0 mM luminol and 50 mM H₂O₂, respectively. CL reaction buffer was 20 mM NaHCO₃ solution (pH 11.0).

3.5. Immunoreaction conditions

To obtain good analytical performance, incubation time of the immunoreaction was investigated. The Ab–AuNP–G-quadruplex/hemin DNAzyme and CA19-9 mixture was incubated at 37 °C for 30–80 min. The solution was then separated by CE–CL. With the increasing incubation time, the CL intensity (peak height) of Ag–Ab–AuNP–G-quadruplex/hemin complex rapidly increased and reached to the maximum value at 60 min. For further studies 60 min was chosen as the incubation time.

3.6. Optimization of CE conditions

In order to achieve a quick CE separation of Ab–AuNP–G-quadruplex/hemin from Ag–Ab–AuNP–G-quadruplex/hemin complex chemical compositions of the CE running buffer was investigated. In this work, borate buffer was chosen as the running buffer. The buffer concentration was tested from 5 to 25 mM. It was found that best separation results were obtained with 10 mM borate buffer. In order to decrease the adsorption of protein on the capillary inner wall, Tween 20 was used as a capillary inner wall dynamic coating reagent in this work. Tween 20 concentration ranging from 0.08% to 0.5% (v/v) was tested. Results indicated 0.2% Tween 20 in the buffer was enough to prevent protein adsorption. The pH of running buffer has an important effect on the capillary wall surface characteristics and the effective electric charge of the analytes. Generally, protein separation is carried out in an alkaline running buffer. Therefore, the effects of running buffer pH were

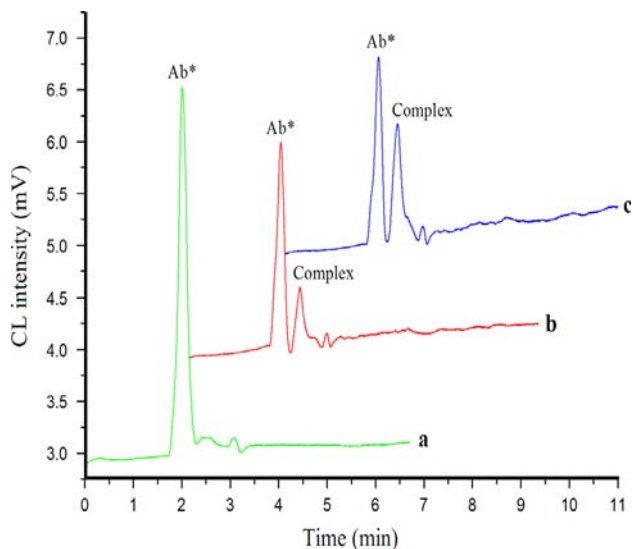


Fig. 5. Electropherograms obtained from separating Ab–AuNP–G–quadruplex/hemin solution (a) and immunoreaction solution of Ab–AuNP–G–quadruplex/hemin with CA19-9 at 0.25 (b) and 0.60 U/mL (c) CL reaction buffer was 20 mM NaHCO₃ solution (pH 11.0) containing 1.0 mM luminol and 50 mM H₂O₂. Running buffer was 10 mM borate buffer (pH 10.0) containing 0.2% (v/v) Tween 20. Separation voltage was 20 kV. Sample was injected hydrodynamically at 20 cm for 8 s.

investigated in a weak alkaline range. It was found that resolution value increased with the increase of running buffer pH from 8.5 to 10.0, and then decreased with further increase in buffer pH from 10.0 to 11.0. Therefore, pH 10.0 of the running buffer was chosen for further experiments.

Based on the experimental results described above, the best conditions for CE separation of Ab–AuNP–G–quadruplex/hemin and Ag–Ab–AuNP–G–quadruplex/hemin complex were confirmed as following: 20 kV separation voltage and a running buffer at pH 10.0 containing 10 mM borate buffer and 0.2% Tween 20. Fig. 5 shows typical electropherograms obtained from the noncompetitive immunoassay of CA19-9 under the optimized conditions. It can be seen from the electropherograms that the free Ab–AuNP–G–quadruplex/hemin and the immunocomplex were separated from each other within 3 min. It also can be seen that the peak height for immunocomplex increased with increase in CA19-9 concentration (Fig. 5b for 0.25 U/mL and Fig. 5c for 0.60 U/mL CA19-9).

3.7. Analytical performance

The analytical performance of the proposed CE-CLIA was evaluated in terms of response linearity, the limit of detection, and the repeatability (precision) of migration times and peak area. In these experiments, the peak area was used for the quantification of CA19-9. To assess the linearity and limit of detection, a series of CA19-9 standard solutions were analyzed. The results indicated that the peak area of the Ag–Ab–AuNP–DNAzyme immunocomplex were directly proportional to the concentrations of CA19-9 in the range 0.025–1.00 U/mL. Linear regression analysis of the results yielded the following equation: $\Delta A = 25.0395C + 0.01418$, $R^2 = 0.9958$. Where ΔA was the peak area of the complex (mV s), and C was the concentration of CA19-9 (U/mL). Amounts of CA19-9 in the human serum samples were calculated from the regression equation. The limit of detection was estimated to be 0.016 U/mL (signal/noise=3), which was more sensitive than many of the CA19-9 assays ever reported (Table 1). The limit of quantitation was estimated to be 0.053 U/mL. Reproducibility (RSD) of the migration time and peak area from assaying a

Table 1
Comparison of analytical methods for CA19-9 quantification.

Method	Linear range (U/mL)	Detection limit (U/mL)	Refs.
EA	3–20	2.68	[36]
EA	2–30	1.37	[37]
EA	0.15–150	0.06	[38]
FA	1–180	0.25	[39]
FA	3.0–500	2.30	[40]
QCM	12.5–270.0	8.3	[41]
RIA	5.8–120	1.4	[42]
FIA-CL	2–25	1.0	[43]
CLEIA		390	[44]
CE-CLIA	0.025–1.0	0.016	This work

EA, electrochemical assay; FA, fluorometric assay; QCM, Quartz crystal microbalance-based assay; RIA, radioimmunoassay; FIA, flow injection assay; EIA, enzyme-linked immunoassay.

0.08 U/mL CA19-9 standard solution ($n=5$) were 0.62% and 2.8%, respectively.

3.8. Determination of CA19-9 in human serum

The potential of the proposed CE-CLIA method in clinical applications was preliminarily evaluated by analyzing human serum samples whose CA19-9 contents were determined in a hospital's clinic lab by using an established ELISA method. Five samples, three from subjects with benign conditions and two from cancer patients were analyzed. Electropherograms obtained from each group are shown in Fig. 6. It can be seen from the electropherograms that free Ab–AuNP–G–quadruplex/hemin and the complex were well separated within 3 min. Peak identifications were verified by spiking the sample with authentic compounds. Analytical results for five serum samples analyzed are summarized in Table 2. As can be seen, CA19-9 levels measured in normal serum samples were around <21.3 U/mL which was in consistency with the reference value established in clinical practice (i.e. <35 U/mL). In patient serum samples, the CA19-9 level was found to be >55.4 U/mL, which was obviously higher than the reference value. The precisions of method (RSD) were in the range of 2.8–4.8%. Further, the results found by the proposed CE-CLIA method compared well with the results obtained by the hospital clinic lab using an ELISA method. To further assess the feasibility of the proposed method to analyze human serum samples, recovery of CA19-9 from this sample matrix was studied by adding CA19-9 at three different levels (5.0, 10, and 50 U/mL) into the serum samples. Recovery results were found to be in the range of 96.0–105.0% (shown in Table 3). These results indicated that the present CE-CLIA method was reliable for analysis of CA19-9 in human serum and useful in clinical applications.

4. Conclusion

A novel strategy of analytical signal amplification in CE-CLIA by means of an antibody–AuNP–DNAzyme assembly was demonstrated. The nano-meter sized assembly was prepared via electrostatic immobilization of antibody and covalent binding of HS-DNA at a molar ratio of multiple times to the antibody onto the AuNP. Hemin was embedded in the guanine-rich DNA strand after K⁺ induced folding, forming a G–quadruplex/hemin DNAzyme. Due to the DNAzyme's high CL catalytic efficiency and a high loading ratio of the DNAzyme over the signal antibody on AuNP surface, analytical signal amplification was achieved. Deploying this novel signal amplification strategy, an ultrasensitive CE-CLIA method for quantifying CA19-9, an important cancer biomarker, was developed with a detection limit of 0.016 U/mL CA19-9, the lowest ever

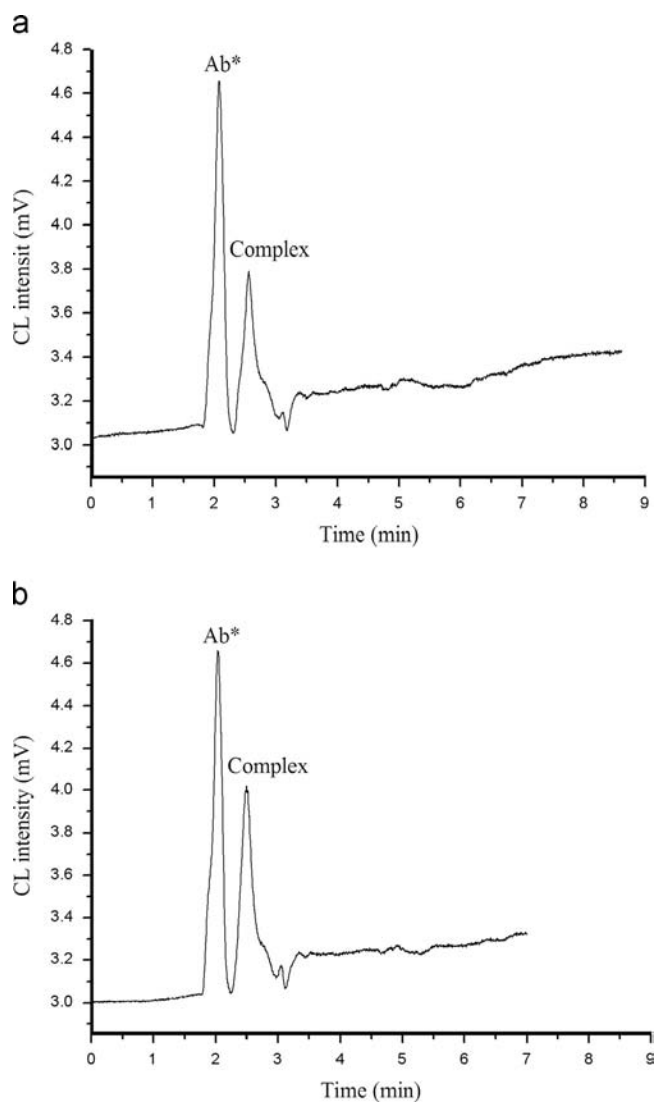


Fig. 6. Electropherograms obtained from analysis of human serum samples: (a) sample taken from a normal subject (10-times dilution) and (b) sample taken from a cancer patient (100-times dilution), indicating a much higher CA 19-9 level in the patient serum. Experimental conditions were as in Fig. 5.

Table 2
Analytical results of CA19-9 in human serum samples.

Sample	Found by present method (U/mL)	RSD (% , n=5)	Found by ELISA* (U/mL)
Healthy subject 1	7.7	4.4	7.9
Healthy subject 2	21.3	4.8	19.2
Healthy subject 3	4.6	3.0	4.8
Cancer patient 1	55.4	2.8	54.6
Cancer patient 2	62.9	2.8	63.3

* Results obtained by a hospital clinic lab using an established ELISA method.

reported. The method was applied for the determination of CA19-9 in human serum samples. The analytical results were in a good agreement with those obtained by using an established ELISA method. In contrast to traditional immunoassay, the present CE-CLIA method is simple in design and fast in operation. The simple operation can avoid the multiple procedures of traditional immunoassay and washing steps, and subsequently reduce the errors and deviations caused inevitably by those steps. It is expected that the signal amplification concept proved in this work

Table 3
Recovery study for the proposed CE-CLIA assay of CA19-9.

Serum Sample	CA19-9 concentration (U/mL)	CA19-9 added (U/mL)	CA19-9 measured (U/mL)	Recovery (%)
#1	7.7	5.0	12.8	102.0
		10	17.3	96.0
		50	57.9	100.4
#2	21.3	5.0	26.2	98.0
		10	31.8	105.0
		50	69.9	97.2

is useful for CL immunoassays of other antigens by using respective antibodies, and thus affords a new avenue to ultrasensitive determination of biomolecules for early disease diagnosis.

Acknowledgments

Financial support from National Natural Science Foundation of China (no. 21175030 to SZ), and US National Institutes of Health (GM089557 to YML) is gratefully acknowledged.

References

- A.M. García-Campana, F.J. Lara, L. Gamiz-Gracia, J.F. Huertas-Perez, *TrAC–Trends Anal. Chem.* 28 (2009) 973–986.
- Y. Weizmann, Z. Cheglakov, I. Willner, *J. Am. Chem. Soc.* 130 (2008) 17224–17225.
- X. Ji, Z. He, X. Ai, H. Yang, C. Xu, *Talanta* 70 (2006) 353–357.
- R.G. Nielsen, E.C. Rickard, P.F. Santa, D.A. Sharknas, G.S. Sittampalam, *J. Chromatogr. A* 539 (1991) 177–185.
- J.J. Bao, *J. Chromatogr. A* 699 (1997) 463–480.
- A.C. Moser, D.S. Hage, *Electrophoresis* 29 (2008) 3279–3295.
- Y.M. Liu, L. Mei, L.J. Liu, L.F. Peng, Y.H. Chen, S.R. Ren, *Anal. Chem.* 83 (2011) 1137–1143.
- Y.L. Luo, Y.S. Shiao, Y.F. Huang, *ACS Nano* 5 (2011) 7796–7804.
- Y. Chen, M.B. O'Donoghue, Y.F. Huang, H. Kang, J.A. Phillips, X. Chen, M.C. Estevez, C.J. Yang, W. Tan, *J. Am. Chem. Soc.* 132 (2010) 16559–16570.
- S. Bi, Y.M. Yan, X.Y. Yang, S.S. Zhang, *Chem. Eur. J.* 15 (2009) 4704–4709.
- Q.F. Li, D.P. Tang, J. Tang, B.L. Su, J.X. Huang, G.N. Chen, *Talanta* 84 (2011) 538–546.
- R. Elghanian, J.J. Storchhoff, R.C. Mucic, R.L. Letsinger, C.A. Mirkin, *Science* 277 (1997) 1078–1081.
- Y.C. Cao, R.C. Jin, J.M. Nam, C.S. Thaxton, C.A. Mirkin, *J. Am. Chem. Soc.* 125 (2003) 14676–14677.
- X. Yang, J. Xu, X. Tang, H. Liu, D. Tian, *Chem. Commun.* 46 (2010) 3107–3109.
- J. Zhang, S. Song, L. Zhang, L. Wang, H. Wu, D. Pan, C. Fan, *J. Am. Chem. Soc.* 128 (2006) 8575–8580.
- V. Pavlov, Y. Xiao, B. Shlyahovsky, I. Willner, *J. Am. Chem. Soc.* 126 (2004) 11768–11769.
- X.C. Zhou, S.J. O'Shea, S.F.Y. Li, *Chem. Commun.* (2000) 953–954.
- S. Bi, H. Zhou, S. Zhang, *Chem. Commun.* (2009) 5567–5569.
- S. Bi, H. Zou, S. Zhang, *Chem. Sci.* 1 (2010) 681–687.
- E. Golub, G. Pelossof, R. Freeman, H. Zhang, I. Willner, *Anal. Chem.* 81 (2009) 9291–9298.
- M. Deng, D. Zhang, Y. Zhou, X. Zhou, *J. Am. Chem. Soc.* 130 (2008) 13095–13102.
- D. Li, B. Shlyahovsky, J. Elbaz, I. Willner, *J. Am. Chem. Soc.* 129 (2007) 5804–5805.
- T. Li, E. Wang, S. Dong, *Anal. Chem.* 82 (2010) 1515–1520.
- Z. Zhou, Y. Du, L. Zhang, S. Dong, *Biosens. Bioelectron.* 34 (2012) 100–105.
- B. Qiu, Z.Z. Zheng, Y.J. Lu, Z.Y. Lin, K.Y. Wong, G.N. Chen, *Chem. Commun.* 47 (2011) 1437–1439.
- S. Zhang, Z.S. Wu, L. Qiu, H. Zhou, G. Shen, R. Yu, *Chem. Commun.* 46 (2010) 3381–3383.
- S.L. Zhao, C. Xie, X. Lu, Y.R. Song, Y.M. Liu, *Electrophoresis* 26 (2005) 1744–1749.
- S. Zhao, J. Wang, F. Ye, Y.M. Liu, *Anal. Biochem.* 378 (2008) 127–131.
- Y. Zhao, S. Zhao, J. Huang, F. Ye, *Talanta* 85 (2011) 2650–2654.
- T. Li, B.L. Li, S.J. Dong, *Anal. Bioanal. Chem.* 389 (2007) 887–893.
- A. Ambrosi, M.T. Castaneda, A.J. Killard, M.R. Smyth, S. Alegret, A. Merkoci, *Anal. Chem.* 79 (2007) 5232–5240.
- C. Wang, J. Wu, C. Zong, H.X. Ju, F. Yan, *Analyst* 136 (2011) 4295–4300.

- [33] E.M. Rezler, J. Seenisamy, S. Bashyam, M.Y. Kim, E. White, W.D. Wilson, L.H. Hurley, *J. Am. Chem. Soc.* 127 (2005) 9439–9447.
- [34] D.M. Kong, J. Wu, N. Wang, W. Yang, H.X. Shen, *Talanta* 80 (2009) 459–465.
- [35] Y. Lu, J. Liu, *Acc. Chem. Res.* 40 (2007) 315–323.
- [36] D. Du, F. Yan, S.L. Liu, H.X. Ju, *J. Immunol. Methods* 283 (2003) 67–75.
- [37] D. Du, X.X. Xu, S.F. Wang, A.D. Zhang, *Talanta* 71 (2007) 1257–1262.
- [38] Y. Zhuo, R. Yuan, Y.Q. Chai, C.L. Hong, *Analyst* 135 (2010) 2036–2042.
- [39] B.X. Gu, C.X. Xu, C. Yang, S.Q. Liu, M.L. Wang, *Biosens. Bioelectron.* 26 (2011) 2720–2723.
- [40] Y.J. Zhao, X.W. Zhao, X.P. Pei, J. Hua, W.J. Zhao, B. Chen, Z.Z. Gu, *Anal. Chim. Acta* 633 (2009) 103–108.
- [41] Y.J. Ding, J. Liu, X.Y. Jin, H.X. Lu, G.L. Shen, R.Q. Yu, *Analyst* 133 (2008) 184–190.
- [42] B.C.D. Villano, S. Brennan, P. Brock, C. Bucher, V. Liu, M. McClure, B. Rake, S. Space, B. Westrick, H. Schoemaker, V.A. Zurawski, *Clin. Chem.* 29 (1983) 549–552.
- [43] J.H. Lin, F. Yan, X.Y. Hu, H.X. Ju, *J. Immunol. Methods* 291 (2004) 165–174.
- [44] I. Nishizono, S. Iida, N. Suzuki, H. Kawada, H. Murakami, Y. Ashihara, M. Okada, *Clin. Chem.* 37 (1991) 1639–1644.